Climatic Change (2024) 177:109
https://doi.org/10.1007/s10584-024-03766-7

A time of emergence (TOE) analysis on the impact and uncertainty of global warming on Korean peak summers

Jihun Ryu[1] · Shih-Yu (Simon) Wang[2] · Jin-Ho Yoon[1]

Received: 22 November 2023 / Accepted: 12 June 2024

Abstract
In recent years, South Korea has experienced a notable escalation in the intensity and frequency of summer heat. To quantitatively gauge the impact of global warming on Korean summers, this study employs the Time of Emergence (TOE) method, assessing when the effects of global warming surpass natural climate variability. Determining a precise regional TOE is challenging due to disparities between modeled climates and observations. For peak summer seasons (July and August), TOE estimates range from the 2010s to the early 2030s in Shared Socioeconomic Pathways (SSP) 5-8.5, suggesting an imminent or already reached TOE. However, for the same scenario, different methodologies and datasets project the TOE to the late 21st century, suggesting the existence of uncertainty in the TOE. One reason for this uncertainty is the discrepancies identified between climate models and observations, which suggest that climate models could delay the TOE beyond the present time. Furthermore, from 1959 to 2014, global warming accounts for less than 10% of the observed temperature. Despite this, the strengthening of global warming signals is confirmed, leading to the expectation of more extreme events than those seen in the 2018 heat wave. This raises questions about current estimates of TOE and emphasizes the need for robust climate modeling to inform effective climate action.

Keywords Climate change · Natural climate variability · Long-term trend · Time of emergence

1 Introduction

In terms of hotter summers, a pivotal question frequently raised by both the media and the scientific community pertains to the extent to which global warming contributes to a region's heightened temperatures. In the context of Korea's warmest summer on record in

✉ Jin-Ho Yoon
yjinho@gist.ac.kr

1 School of Earth Sciences and Environmental Engineering, Gwangju Institute of Science and Technology, Gwangju, South Korea

2 Department of Plants Soil and Climate, Utah State University, Logan, UT, USA

2018, anthropogenic forcing may have augmented the likelihood of such an extreme heat wave by at least fourfold, considering both intensity and maximum duration (Min et al. 2020). While the causative factors for these extremes remain a topic of debate, the impacts of global warming are markedly pronounced in South Korea. The annual mean temperature of South Korea has risen by over 1ºC at a rate of 0.23ºC per decade from 1954 to 1999, surpassing the global mean air temperature increase (Hansen et al. 2006; Jung et al. 2002). Projected estimates indicate a potential rise of 4.8 ± 1.11ºC in Korea's annual mean temperature by 2100, based on the Representative Concentration Pathway 8.5 (RCP8.5) scenario (KMA 2014). To contextualize the summer heat wave of 2018 in Korea, it approximates conditions akin to a 3ºC global warming increase (Im et al. 2019).

Natural climate variability undeniably exerts a significant influence on Korean summer temperatures. Notably, two distinct atmospheric circulation patterns have been identified concerning heat waves: (1) zonal and (2) meridional wave types (Yeo et al. 2019). The former is characterized by a large-scale atmospheric teleconnection pattern across the Eurasian continent, while the latter is linked to convection in the subtropical northwestern Pacific Ocean. The noteworthy hot summers of 2015 and 2016 were attributed to meridional wave types (Yeh et al. 2018; Yoon et al. 2018), whereas the heatwave in 1994 was associated with a large-scale atmospheric circulation connected to the Eurasian continent (Ha et al. 2020; Yeo et al. 2019).

To quantify the relative contributions of global warming and natural climate variability to the occurrence of extremely hot summers, various approaches have been tested (Angélil et al. 2014; Schär et al. 2004; Stott et al. 2004). Among these approaches, the Time of Emergence (TOE), a concept introduced by Hawkins and Sutton in 2012, is defined as the point at which the signal of a specific climate variable, such as temperature, exceeds the range of natural climate variability. It has been adopted in subsequent studies (Mahlstein et al. 2011; Maraun 2013; Mora et al. 2013). to gauge the effect of global warming. The TOE analysis is effective because it identifies when the signals of climate warming become statistically distinguishable from natural variability. This critical insight enables us to forecast with greater confidence the timeline for significant climate impacts, allowing for more effective and timely policy interventions. Specifically, TOE helps in pinpointing vulnerabilities, facilitating targeted adaptation strategies before the impacts become irreversible. TOE is frequently calculated based on the Coupled Model Intercomparison Project Phase 5 (CMIP5) and Phase 6 (CMIP6). On a global scale, the TOE was estimated to occur around the 2000s in CMIP5 models based on RCP 8.5 (Hyun et al. 2020). Previous research indicates tropical TOE emergence before 2020, while in extra-tropical regions, it is anticipated after 2030 (Hawkins and Sutton 2012). In Korea, the TOE for daily maximum and minimum temperatures during the summer season is estimated around the 2040s (Lee et al. 2016).

One factor contributing to the divergence in TOE estimations can be discrepancies between observations and climate models of natural climate variability and global warming trends. Despite advancements in state-of-the-art climate models, reported biases in temperature, including uncertainties in simulating natural climate variability, persist (Masson-Delmotte et al. 2021). Notable uncertainties are found in the simulation of natural climate variability (e.g., Hawkins and Sutton 2009; Deser et al. 2012; Thompson et al. 2015). Probabilistic diagnostics employing multi-model or multi-ensemble approaches have been utilized to objectively depict climate model biases. To address these challenges, it has been proposed to simultaneously use CMIP5, with its multiple models, and the Community Earth

System Model version 1's Large Ensemble (CESM1-LE), incorporating multiple ensembles, to estimate natural variability(Deser et al. 2016).

This study investigated the TOE of Korean summer temperature, the point at which it will transition from the current climate to a new normal driven by global warming. We utilized an observation-based statistical model to predict the regional TOE, integrating these observations with model projections to quantitatively assess when and what these changes will be. We also examined how natural climate variability and long-term trends depicted in climate models affect the accuracy and potential biases of these TOE estimates. This integrated approach, an improvement from previous methods and therefore considered innovative, is crucial for developing effective mitigation strategies. In Sect. 2, we provide a detailed description of the data and methods employed. Section 3 comprehensively explores and discusses the regionally distributed TOE, highlighting disparities in natural climate variability and long-term temperature trends. The study concludes with Sect. 4, which offers final remarks and discussions on the findings.

2 Data and methods

2.1 Data

The pivotal data in this study encompasses monthly temperature records, drawing on various datasets spanning the period from 1959 to 2014. Initially, temperature data were sourced from seven Korea Meteorological Administration (KMA) stations. Additionally, data from the Climatic Research Unit (CRU), interpolated based on station observations, were incorporated (Harris et al. 2020). Reanalysis temperature data sets from the Japanese 55-year Reanalysis (JRA-55), the 20th-century reanalysis V3 (20CRV3), the fifth-generation European Centre for Medium-Range Weather Forecasts reanalysis (ERA5), and the National Centers for Environmental Prediction/National Center for Atmospheric Research Reanalysis 1 (NCEP R1) were also utilized (Compo et al. 2011; Hersbach et al. 2020; Kalnay et al. 2018; Poli et al. 2016; Slivinski et al. 2019). The horizontal resolutions of CRU, JRA-55, 20CRV3, ERA5, and NCEP R1 are $0.5^{o} \times 0.5^{o}$, $1.25^{o} \times 1.25^{o}$, $1^{o} \times 1^{o}$, $0.25^{o} \times 0.25^{o}$, and T62 grid, respectively.

The monthly surface air temperatures were acquired from multiple models within the CMIP6 archives: 39 models in SSP2-4.5 and 42 models in SSP5-8.5 for CMIP6 (Eyring et al. 2016). For extension purposes, only models with the same ensemble number (r1i1p1f1) were utilized, with varying model numbers for each scenario. A single ensemble member was exclusively employed due to its advantages in representing extremes, as opposed to a multi-model mean (Knutti et al. 2010). Both historical simulations spanning 1959–2014 and future projection simulations from 2015 to 2099 were incorporated from CMIP6. In addition, we used monthly surface air temperatures from CMIP6's hist-GHG and hist-aer scenarios for 14 and 12 models, respectively. These were only used for the period 1959–2014 to determine the impact of aerosols, which are a localized component. The climate models included the historical, SSP2-4.5, SSP5-8.5, hist-GHG, and hist-aer used are detailed in Tables S1 and S2.

Additionally, four models—Community Earth System Model 2 Large Ensemble (CESM2-LE) (Rodgers et al. 2021), the sixth version of the Model for Interdisciplinary

Research on Climate (MIROC6) (Tatebe et al. 2019), the Canadian Earth System Model version 5 (CanESM5) (Swart et al. 2019), and EC-Earth3 (Döscher et al. 2021)—were selected to employ multiple ensembles within a single model. CESM2-LE, MIROC6, CanESM5, and EC-Earth3 were chosen to verify the accurate simulation of natural variability and trends by the current climate model. The number of ensembles used for CESM2-LE, MIROC6, CanESM5, and EC-Earth3 were 50, 50, 25, and 22, respectively. In particular, MIROC6 and CanESM5 were also utilized for TOE prediction, utilizing the SSP2-4.5 and SSP5-8.5 scenarios.

Monthly atmospheric CO_2 concentrations and gridded SO_2 emissions were employed to approximate the long-term temperature trend. The CO_2 concentrations were sourced from the Mauna Loa observatory provided by the National Oceanic and Atmospheric Administration (NOAA) (Keeling et al. 2005). The gridded SO_2 emissions are available in the input datasets for Model Intercomparison Projects (input4MIPS) (Hoesly et al. 2018). Specifically, historical emissions and forced emissions from the SSP2-4.5 and SSP5-8.5 scenarios were utilized.

2.2 Methods

The Korean temperature and the global temperature were defined in this study. For Korean temperatures, the arithmetic average of air temperature from seven KMA stations (KMA7) served as the ground data, and the grid data were area-averaged over 34°–38°N and 125°–130°E after masking out the ocean (Min et al. 2020). Regarding global temperature, the grid data were globally area-averaged after excluding oceanic areas.

The estimation of surface air temperature TOE presents challenges due to various factors, including (i) defining long-term trends influenced by anthropogenic factors and (ii) estimating natural climate variability. Metrics for anthropogenic influences include widely-used methods such as the linear trend method, utilizing atmospheric CO_2 concentrations (Wu et al. 2019), and multimodel ensembles (Dai et al. 2015). Various approaches are employed to estimate natural climate variability, encompassing Thompson's method, methods based on large-scale atmospheric circulation (Dai et al. 2015), and a method based on standard deviation. It is essential to note that there is no clear superiority or inferiority among these methods.

In this study, natural climate variability was defined in two ways. The primary method uses double standard deviations from detrended temperature data, widely recognized as a straightforward indicator of climate variability (Hawkins and Sutton 2012; Lee et al. 2016). In particular, the trend is set to a quadratic trend. Although this method is efficient, it may introduce uncertainties, prompting us to adopt a second approach proposed by a previous study (Thompson et al. 2015). This analytical method refines the standard deviation technique by including autocorrelation, providing a more nuanced understanding of variability and expressed in Eq. (1). The critical t statistic 't_c' used the two-tailed 95% confidence level, and the number of time steps is 'n_t'. 'σ' is the standard deviation of detrended temperature, and '$g\left(n_t\right)$' is the standard deviation of time, '$\gamma\left(n_t, r_1\right)$' is the scaling factor using the lag-one autocorrelation.

$$e = t_c n_t \sigma \gamma\left(n_t, r_1\right) g\left(n_t\right) \tag{1}$$

Next, we need to consider how we can predict the future and explore three methods. The first method employed linear future projections used in previous studies that included "single threshold," one of the methods applied to TOE (Maraun 2013). However, it is well known that the model's future projected temperatures can be affected by various factors and may contain errors or uncertainty, especially on a regional scale (Hawkins and Sutton 2012).

To resolve the uncertainty, statistical models derived from observations were used to predict future temperatures. Two methods were employed: the second and third methods, both decomposing the observed temperature into natural climate variability and anthropogenic factors. The second method uses an anthropogenic factor consisting only of global warming, as shown in Eq. (2). Future temperature trends were simulated using this statistical model, taking into account the CO_2 concentration defined by the RCP scenario. Estimation of the rate of temperature increase based on only CO_2 concentrations was adopted in former research (Callendar 1938). For example, the empirical approximation of Callendar's model reached the lower bound of CMIP5 future projection, and the method of using only CO_2 concentrations can be expected to reduce the uncertainty in the model projection (Anderson et al. 2016). Also, when removing the temperature trend, it was removed with a quadratic trend.

$$T_2 = aT_{detrend} + b\ln(CO_2conc./280) \tag{2}$$

A local forcing effect of anthropogenic aerosols was added in the third method (Eq. (3)). SO_2 emissions, considered precursors of sulfate aerosols with a cooling effect, were used as a local forcing effect. The term $[b\ln(CO_2conc./280) - cSO_2emis.]$ containing both global warming and local forcing effect, was used for the third future projection in Eq. (3).

$$T_3 = aT_{detrend} + b\ln(CO_2conc./280) - cSO_2emis. \tag{3}$$

The statistical model in Eqs. (2) and (3) allows us to quantify the contributions of natural variability, global warming, and the local aerosol effect. Coefficients within this equation were used to analyze these contributions. Using Eq. (3) as an example, we standardized each variable to express the equation as shown in Eq. (4), where a', b', and c' are dimensionless coefficients representing the contributions of natural variability, global warming, and local forcing effects, respectively, as shown in Eq. (5).

$$\frac{T}{\sigma_T} = a\frac{\sigma_{T_{detrend}}}{\sigma_T}\frac{T_{detrend}}{\sigma_{T_{detrend}}} + b\frac{\sigma_{\ln(CO_2conc./280)}}{\sigma_T}\frac{\ln(CO_2conc./280)}{\sigma_{\ln(CO_2conc./280)}} - c\frac{\sigma_{SO_2emis.}}{\sigma_T}\frac{SO_2emis.}{\sigma_{SO_2emis.}} \tag{4}$$

$$a' = a\frac{\sigma_{T_{detrend}}}{\sigma_T}, b' = b\frac{\sigma_{\ln(CO_2conc./280).}}{\sigma_T}, c' = c\frac{\sigma_{SO_2emis.}}{\sigma_T} \tag{5}$$

To comprehensively assess the impact of anthropogenic factors, we employed the TOE by integrating natural climate variability and long-term trends. Natural climate variability was defined based on the Thompson method and double standard deviations. Long-term trends were defined as a linear future projection, a global warming term using only CO_2 concentration, and a term that takes into account both global warming and local factors, where both CO_2 concentration and SO_2 emissions were considered. In the case of natural climate variability, previous studies (e.g., Hawkins and Sutton 2012; Maraun 2013; Mora et al. 2013) used one or double standard deviations for interannual variability, but here we also used the Thompson method as done by Hyun et al. (2020). As we made future projections using linear trends, CO_2 only, and both CO_2 and SO_2, we used the "single threshold" method.

3 Results and discussion

3.1 Estimation of regional TOE during peak summer in Korea

As global temperatures continue to rise, the contribution of global warming to this increase is expected to become even more significant. The 2018 summer heat wave in South Korea serves as an important example. The summer of 2018, which was reported as an incident only existing in the 3 ºC global warming temperature scenario (Im et al. 2019), lasted four times as long as was simulated without global warming (Min et al. 2020). Other research suggests that it was predominantly driven by atmospheric circulation patterns (Ha et al. 2020). We utilized two methods to measure natural climate variability: Thompson's method and double standard deviations. The long-term trend utilizes a linear trend from each model, calculated by segmenting the historical trend from 1959 to 2014 and the future trend from 2015 to 2099, thereby connecting the two into a single continuous trend with an inflection point between 2014 and 2015.

Figure 1 illustrates two sets of TOEs based on the linear trend for future projections. On the left, the black, blue, and red box plots represent TOEs calculated using the Thompson method for estimating natural climate variability, corresponding to CMIP6, CanESM5, and MIROC6, respectively. On the right, the box plots represent TOEs derived from the double standard deviation method. Additionally, the mean and one standard deviation range of TOEs are indicated as stars and lines next to each boxplot,,and below each TOE boxplot and marker, we list the number of instances in which TOEs were predicted through 2099 for each group. It is noteworthy that the TOE, when estimated based on Thompson's natural variability method, appears about 10 to 20 years earlier than that calculated with the double standard deviation method. Furthermore, the TOE consistently manifests later in the SSP2-4.5 scenario compared to the SSP5-8.5 scenario, emphasizing once again the critical role of reducing greenhouse gas emissions in raising air temperature (see Fig. 1).

According to Thompson's method and the SSP5-8.5 scenario, the TOE has already occurred, and in the SSP2-4.5 scenario, it has either already transpired or is imminent. When utilizing the double standard deviation method, the TOE is projected to occur around 2030 and 2050 for the SSP5-8.5 and SSP2-4.5 scenarios, respectively, with the exception of the projections from the CanESM5 model. Due to its notably strong trend, as highlighted in a prior study (Swart et al. 2019), CanESM5 anticipates a TOE around 2020 and 2027 for the SSP5-8.5 and SSP2-4.5 scenarios, respectively. A previous study (Lee et al. 2016) estimated the TOE to be in the early 2040s, based on the double standard deviation method for estimating natural variability and using signal-to-noise methods, specifically in the context of Northeast Asia during the summer season.

So far, we have fixed a linear trend and explored uncertainty related to natural variability, but now we have analyzed uncertainty concerning the long-term trend. The new methodology involves using long-term trends obtained from statistical models

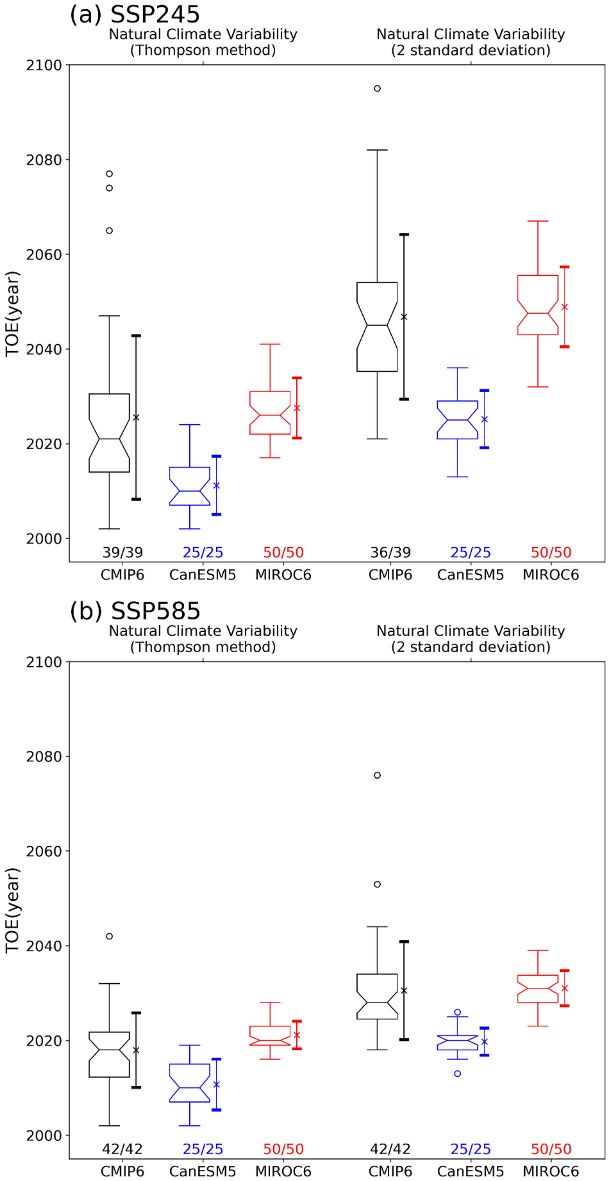

Fig. 1 TOE (Time of Emergence) based on Korean peak summer temperature based on SSP245 in (**a**) and SSP585 in (**b**). The black, blue, and red boxplots represent CMIP6, CanESM5, and MIROC6, respectively. The three box plots on the left use Thompson's method for natural climate variability and the three box plots on the right use double standard deviation. For each plot, stars and lines indicate the mean and standard deviation range next to it, with the number of TOEs predicted versus the sample size shown below

based on KMA7. We used the anthropogenic factor terms $[b\ln(CO_2conc./280)]$ and $[b\ln(CO_2conc./280) - cSO_2emis.]$ in Eqs. (2) and (3), respectively, which are the second and third methods of the long-term trend. The natural climate variability of the reanalysis data was also represented through the natural climate variability term $[aT_{detrend}]$ in Eqs. (2) and (3). The results show a delay in the TOE compared to the linear trend results, especially in the CMIP6 TOE of the SSP5-8.5 scenario using Thompson's natural climate variability, with delays of about 12 years for both global warming and local effects and about 22 years for global warming alone (Figure S1). Additionally, observationally-based TOEs appear later than those in climate models.

These results are further confirmed in Figures S2 and S3 using historical, hist-GHG, and hist-aer scenarios. Figures S2 and S3 depict the annual and seasonal temperatures globally and for Korea, respectively. Both globally and locally, the hist-GHG scenario shows similar distributions to historical scenarios and warming trends, while the hist-aer scenarios have a distinct contribution to the cooling effect. For peak summer in Korea, the historical and hist-GHG scenarios show overall alignment, indicating a predominant GHG influence. Statistically, they are not different groups, but if we compare the means of the scenarios, we see a stronger trend in hist-GHG. Therefore, we used both statistical models to make TOE predictions.

In summary, even for the same future scenario, TOEs can fluctuate significantly depending on how natural climate variability and long-term trends are defined and computed. This indicates that there is still considerable uncertainty in regional TOEs. Moreover, it is difficult to assign superiority to any particular method, making it clear that predicting TOEs using only one specific method risks overestimating or underestimating the impact of climate change. These results are corroborated by previous research suggesting that greater estimated natural climate variability can potentially delay the TOE (Hawkins and Sutton 2012). Therefore, in the following section, biases in the climate models are evaluated with regard to the metrics employed to calculate TOE against reanalysis.

3.2 Biases in simulated natural climate variability and long-term trend

Focusing on the natural climate variability and long-term trend revealed by the widely deployed TOE, we compared surface air temperatures from multiple model single-ensembles in CMIP6 with single model multi-ensembles in CESM2-LE, MIROC6, CanESM5, and EC-Earth3, using several observational datasets. Analyzing peak summer (July-August), which is crucial for assessing heatwave risks in Korea (Kysely and Kim 2009), we found a strong correlation between data from station temperature and reanalysis in Fig. 2(a). To validate our analysis, we utilized a multi-model and multi-ensemble approach, and presented our results through Kernel Density Estimation (KDE) plots in Fig. 2(c) and (d). The graph displays varying results from Thompson's method compared to the double standard deviation approach. Thompson's method indicates that the mean values of natural climate variability in the models and observations are not statistically different, although the models under-simulate the observations by about 6%. In contrast, the double standard deviation approach reveals a statistically significant difference, consistently underestimating natural climate variability.

When examining the long-term trend of peak summer temperatures, the KMA7 temperature indicated an increase of 0.04 ºC per decade from 1959 to 2014, which is lower than the annual averaged value of 0.21 ºC per decade. Although various reanalysis data exhibited similar interannual fluctuations, they depicted different long-term trends. For instance, the strongest trend was observed in KMA7, while the weakest was in JRA-55, even showing a decreasing trend of -0.09 ºC per decade. The ensemble mean linear temperature trends for CMIP6, CESM2-LE, MIROC6, CanESM5, and EC-Earth3 were 0.20, 0.23, 0.12, 0.29, and 0.15 ºC per decade, respectively. When comparing the long-term temperature trends predicted by climate models with those from KMA7, it appears that the models generally

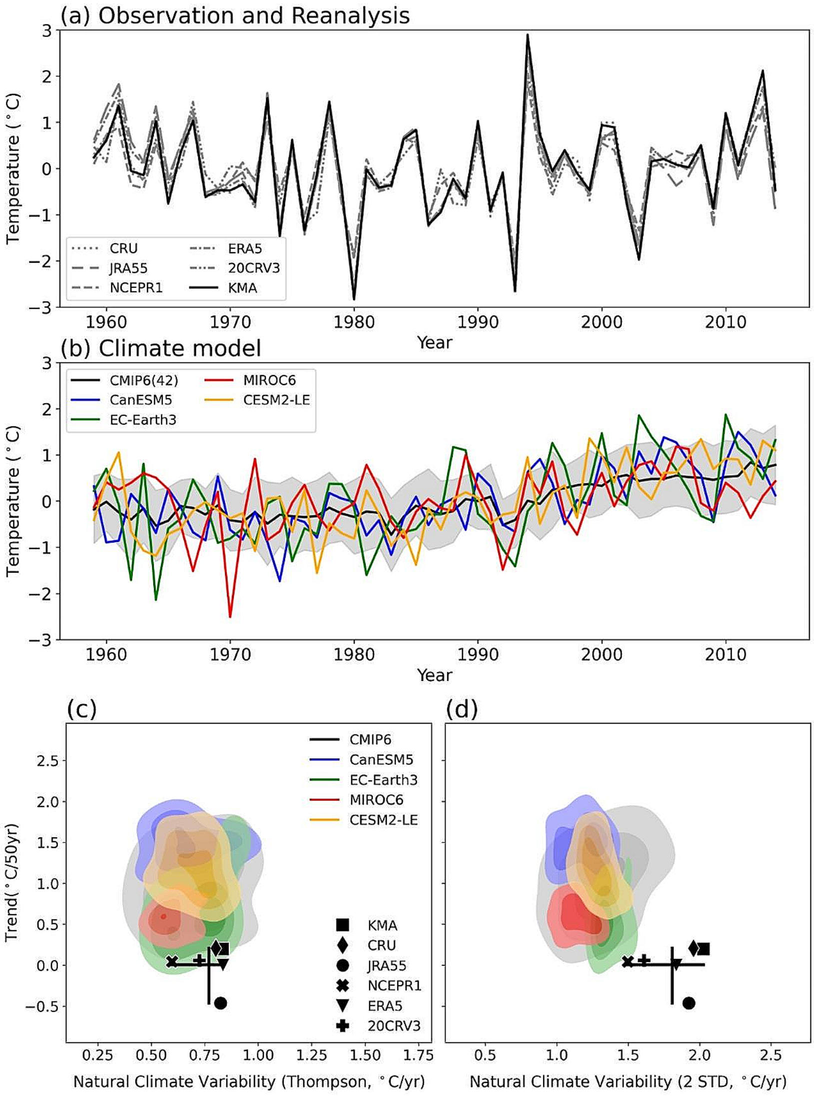

Fig. 2 Time series and KDE plots of Korean peak summer surface air temperature from 1959 to 2014: (**a**) Time series of five reanalysis datasets, (**b**) Time series of model data. The KDE plots illustrating natural climate variability and long-term trends of Korean peak summer surface air temperature are presented in (**c**) and (**d**), respectively. In the KDE plots, the intensity of shading corresponds to the density of the ensemble. (**c**) is Thompson's method and (**d**) is double standard deviations

predict a more pronounced long-term increase. This indicates a potential overestimation of global warming effects in the region by the climate models.

Furthermore, to assess the contributions of natural climate variability and global warming, we standardized each variable and coefficient, as delineated in Eq. (5). In a statistical model considering both global warming and local effects, the contributions to the variation in Korea's peak summer temperatures were estimated to be 9.8% for global warming and 17.8% for local effects. When only global warming was considered, the contribution was 7.9%. This highlights the he TOE for Korean peak summer temperatures has been estimated using significant influence that natural climate variability still has on regional temperature during a particular season. Although natural variability is significant, the established long-term trends point to the likelihood of increasingly extreme temperatures in future Korean summers, surpassing historical records.

Expanding to annual and seasonal trends in Korea, Fig. 3(a) and (b) presents a time series analysis, supporting a conclusion that a single ensemble struggles to capture the nuances of natural climate variability (Figure S4). Continuing with the KDE plots, we observe that CMIP6 tends to overestimate the natural climate variability for annual mean temperature. However, the analysis of seasonal temperatures reveals divergent results (Figure S5). Using the Thompson method, the model results fall within the range of the reanalysis and observations, suggesting a satisfactory simulation across all seasons. In contrast, the double standard deviation method shows overestimation in December-January-February (DJF) and June-July-August (JJA), accompanied by an underestimation in March-April-May (MAM), and an even more pronounced underestimation in September-October-November (SON).

Turning to the long-term trend, the CMIP6 models effectively simulate the temperature increase in South Korea, with 22 out of 42 models falling within the range of reanalysis data and observations, including station observation. A closer examination of seasonal and model-specific multi-ensembles reveals consistent discrepancies between observation and models, particularly during the summer season in Korea. Specifically, the long-term trend is overestimated during the summer, up to more than twice what the observational data indicate, with no ensemble exhibiting a weaker trend than what has been observed. Furthermore, a divergence between Thompson's method and the double standard deviation method emerges when evaluating the natural climate variability during the summer season in Korea. Thompson's method frequently leads to an overestimation compared to observational datasets, while the double standard deviation method tends to result in an underestimation.

Finally, moving to the global scale beyond Korea, the annual average results are displayed in Fig. 4, with the seasonal results shown in Figures S6 and S7. From examining the time series results alone, it appears that the models simulate temperatures adequately, and this consistency extends across all seasons. In the KDE plot of Fig. 4 (c) and (d), it is noteworthy that all climate models exhibit a tendency to overestimate natural climate variability in annual mean temperatures, except for Korea. By applying Thompson's method, only three models align with the range of natural climate variability, increasing to five models when employing the double standard deviation method. These results are in agreement with the reanalysis data. Transitioning to an analysis of the long-term trend, we find that climate models generally tend to slightly overestimate the annual mean trend, aligning with findings from previous research (Dai et al. 2015). The seasonal results mirror the annual trends. Overall, it is evident that climate models commonly overestimate both global natural climate variability and long-term trends.

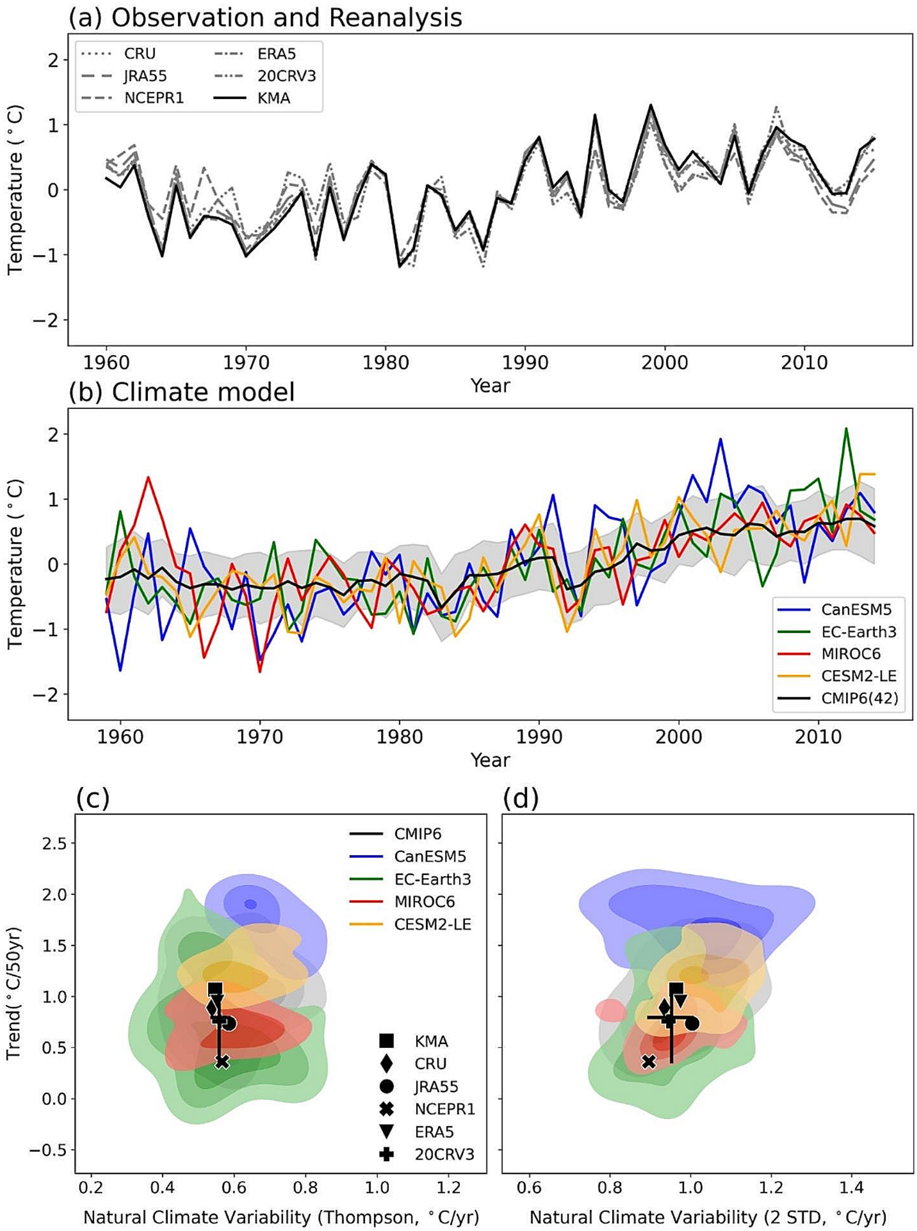

Fig. 3 Same as Fig. 2, but for annual mean temperature over South Korea

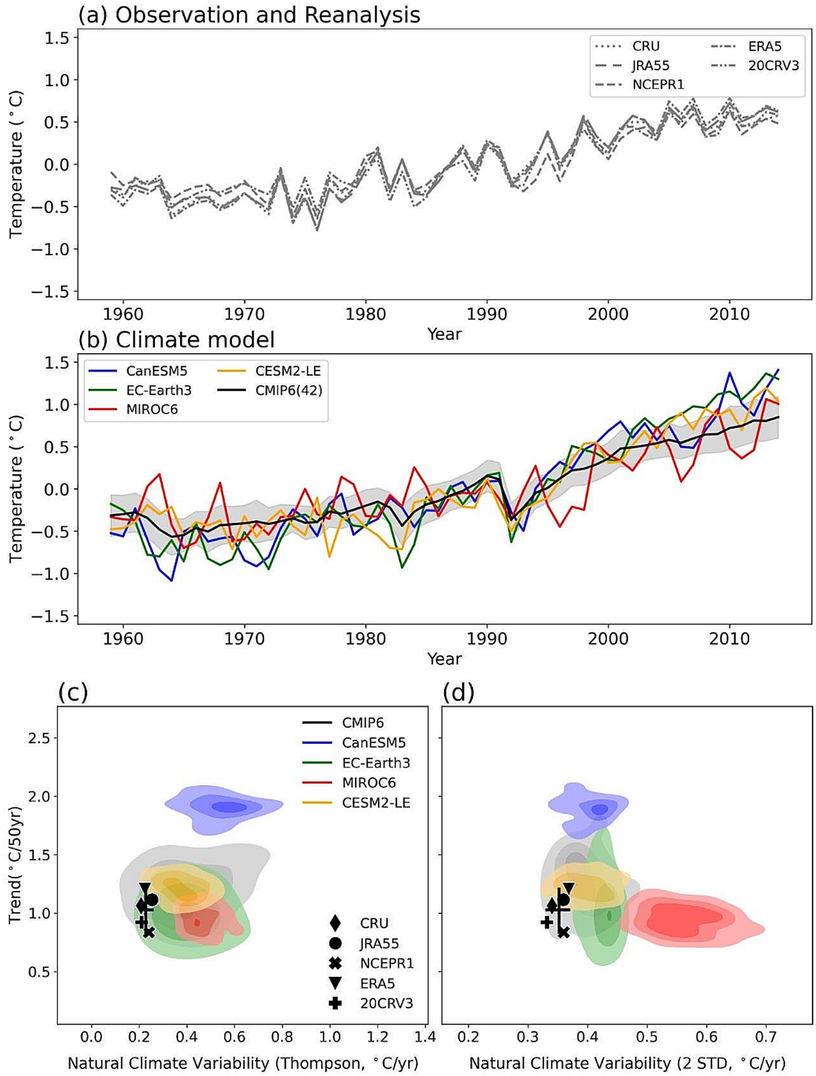

Fig. 4 Same as Fig. 3, but for global annual mean temperature

4 Conclusion

The TOE for Korean peak summer temperatures has been estimated using various methods, some of which have already manifested. For instance, the TOE has been apparent since 2002 in the SSP5-8.5 scenario. On average, the TOE is projected to occur in the 2020s according to the SSP5-8.5 scenarios of the CMIP6 models. Additionally, observation-based statistical models place TOEs approximately 12 or 22 years later than climate models predict, depending on the methodology. No single method has a distinct advantage over the others. However, relying solely on one method is likely to overestimate or underestimate the impact of climate change. Further detailed analyses of the discrepancies between observation-based statistical models and climate models for TOEs were conducted, separating the examination of natural climate variability and long-term trends. This involved utilizing both multi-model single ensembles and single-model multi-ensembles. In our analysis, significant discrepancies between the models' simulations and observed data were identified. For instance, the climate models' simulation of the long-term trend in peak summer temperatures in Korea was about five times larger than the observed trend. Similarly, while the annual mean temperature's long-term trend is well captured by models, they tend to overestimate the natural climate variability. These issues extend globally, with climate models generally overestimating both natural climate variability and long-term trends in global annual mean temperatures.

The observed discrepancies mirror findings in other regions. For example, U.S. summer temperatures and MAM temperatures in India are often overestimated and underestimated, respectively, by climate models (Karrevula et al. 2023; Merrifield and Xie 2016). Furthermore, these models have failed to adequately capture the slowdown in global warming between 2000 and 2013, suggesting a systemic overestimation of global warming (Dai et al. 2015). These regional and global disparities highlight the challenges in accurately predicting TOEs, which are compounded by uncertainties in model physics, scenario variations, internal variability, and the differing importance of models and scenarios across various forecasting periods and regions (Hawkins and Sutton 2009).

Our study also underscores that significant natural climate variability could pose an increased risk during peak summer months, further complicating the challenges of rising temperatures due to anthropogenic greenhouse gas emissions. To address the spread in TOE estimates and improve prediction accuracy, innovative approaches such as the use of artificial neural networks have been proposed (Barnes et al. 2020). These findings emphasize that accurately determining regional TOEs is a critical and ongoing task that requires continued refinement of model predictions and methodologies.

Supplementary Information The online version contains supplementary material available at https://doi.org/10.1007/s10584-024-03766-7.

Acknowledgements This study is funded by the National Research Foundation of Korea and the Korean Meteorological Administration.

Author contributions The study was conceptualized by Jihun Ryu, Shih-Yu (Simon) Wang, and Jin-Ho Yoon. All authors contributed to the methodology and formal analysis. Jihun Ryu has done the data analysis, visualization, and writing the original draft. Reviewing and editing the manuscript is done by Shih-Yu (Simon) Wang, and Jin-Ho Yoon.

Funding This study is funded by the National Research Foundation of Korea under NRF-2021R1A2C1011827 and RS-2023-00283239, the Korean Meteorological Administration Research and Development Program under grant no. KMI2018-07010, and GIST Research Project grant funded by the GIST in 2024. S-Y Wang acknowledges funding from U.S. Department of Energy/Office of Science under Award Number DE-SC0016605 and the U.S. SERDP project RC20-3056.

Data availability The KMA station temperature can be downloaded from https://data.kma.go.kr/. The JRA55 temperature can be downloaded from https://jra.kishou.go.jp/. The CRU temperature can be downloaded from https://crudata.uea.ac.uk/cru/data/hrg/. The 20CR-V3 can be downloaded from https://www.psl.noaa.gov/data/gridded/data.20thC_ReanV3.html. The NCEP R1 temperature can be downloaded from https://psl.noaa.gov/data/gridded/data.ncep.reanalysis.html. The atmospheric CO_2 concentration can be downloaded from https://gml.noaa.gov/ccgg/trends/data.html. The CESM2-LE can be downloaded from https://www.

earthsystemgrid.org/. The CMIP6, CanESM5, MIROC6, EC-Earth3, and SO_2 emission can be downloaded from https://esgf-node.llnl.gov/search/cmip6/.

Declarations

Competing interests The authors declare no competing interests.

References

Anderson TR, Hawkins E, Jones PD (2016) CO2, the greenhouse effect and global warming: from the pioneering work of Arrhenius and Callendar to today's Earth System models. Endeavour 40:178–187

Angélil O, Stone DA, Tadross M, Tummon F, Wehner M, Knutti R (2014) Attribution of extreme weather to anthropogenic greenhouse gas emissions: sensitivity to spatial and temporal scales. Geophys Res Lett 41:2150–2155

Barnes EA, Toms B, Hurrell JW, Ebert-Uphoff I, Anderson C, Anderson D (2020): Indicator patterns of forced change learned by an artificial neural network. *Journal of Advances in Modeling Earth Systems*, 12, e2020MS002195

Callendar GS (1938) The artificial production of carbon dioxide and its influence on temperature. Q J R Meteorol Soc 64:223–240

Compo GP, Coauthors (2011) The twentieth century reanalysis project. Q J R Meteorol Soc 137:1–28

Dai A, Fyfe JC, Xie S-P, Dai X (2015) Decadal modulation of global surface temperature by internal climate variability. Nat Clim Change 5:555–559

Deser C, Terray L, Phillips AS (2016) Forced and internal components of winter air temperature trends over North America during the past 50 years: mechanisms and implications. J Clim 29:2237–2258

Deser C, Phillips A, Bourdette V, Teng H (2012) Uncertainty in climate change projections: the role of internal variability. Climate Dynamics https://link.springer.com/article/10.1007/s00382-010-0977-x

Döscher R, Coauthors (2021) The EC-earth3 Earth system model for the climate model intercomparison project 6. Geoscientific Model Dev Discuss 2021:1–90

Eyring V, Bony S, Meehl GA, Senior CA, Stevens B, Stouffer RJ, Taylor KE (2016) Overview of the coupled model Intercomparison Project Phase 6 (CMIP6) experimental design and organization. Geosci Model Dev 9:1937–1958

Ha K-J, Coauthors (2020) What caused the extraordinarily hot 2018 summer in Korea? J Meteorological Soc Japan Ser II 98:153–167

Hansen J, Sato M, Ruedy R, Lo K, Lea DW, Medina-Elizade M (2006) Global temperature change. Proc Natl Acad Sci 103:14288–14293

Harris I, Osborn TJ, Jones P, Lister D (2020) Version 4 of the CRU TS monthly high-resolution gridded multivariate climate dataset. Sci data 7:109

Hawkins E, Sutton R (2009) The potential to narrow uncertainty in regional climate predictions. Bull Am Meteorol Soc 90:1095–1108

Hawkins E, Sutton R (2012): Time of emergence of climate signals. Geophys Res Lett, 39

Hersbach H, Coauthors (2020) The ERA5 global reanalysis. Q J R Meteorol Soc 146:1999–2049

Hoesly RM, Coauthors (2018) Historical (1750–2014) anthropogenic emissions of reactive gases and aerosols from the Community Emissions Data System (CEDS). Geosci Model Dev 11:369–408

Hyun SH, Yeh SW, Song SY, Park HS, Kirtman BP (2020): Understanding intermodel diversity when simulating the time of emergence in CMIP5 climate models. Geophys Res Lett, 47, e2020GL087923.

Im E-S, Thanh N-X, Kim Y-H, Ahn J-B (2019) 2018 summer extreme temperatures in South Korea and their intensification under 3° C global warming. Environ Res Lett 14:094020

Jung HS, Choi Y, Oh JH, Lim GH (2002) Recent trends in temperature and precipitation over South Korea. Int J Climatology: J Royal Meteorological Soc 22:1327–1337
Kalnay E, Coauthors (2018) The NCEP/NCAR 40-year reanalysis project. Renewable energy. Routledge, Vol1_146-Vol141_194
Karrevula NR, Ramu DA, Nageswararao M, Rao AS (2023) Inter-annual variability of pre-monsoon surface air temperatures over India using the North American Multi-model Ensemble models during the global warming era. Theoret Appl Climatol 151:133–151
Keeling CD, Piper SC, Bacastow RB, Wahlen M, Whorf TP, Heimann M, Meijer HA (2005) Atmospheric CO2 and 13CO2 exchange with the terrestrial biosphere and oceans from 1978 to 2000: observations and carbon cycle implications. A history of atmospheric CO2 and its effects on plants, animals, and ecosystems. Springer, pp 83–113
KMA (2014): Korean Climate Change Assessment Report 2014, 323 pp
Knutti R, Furrer R, Tebaldi C, Cermak J, Meehl GA (2010) Challenges in combining projections from multiple climate models. J Clim 23:2739–2758
Kysely J, Kim J (2009) Mortality during heat waves in South Korea, 1991 to 2005: how exceptional was the 1994 heat wave? Climate Res 38:105–116
Lee D, Coauthors (2016) Time of emergence of anthropogenic warming signals in the Northeast Asia assessed from multi-regional climate models. Asia-Pac J Atmos Sci 52:129–137
Mahlstein I, Knutti R, Solomon S, Portmann RW (2011) Early onset of significant local warming in low latitude countries. Environ Res Lett 6:034009
Maraun D (2013) When will trends in European mean and heavy daily precipitation emerge? Environ Res Lett 8:014004
Masson-Delmotte V, Coauthors (2021): Climate change 2021: the physical science basis. *Contribution of working group I to the sixth assessment report of the intergovernmental panel on climate change*, 2
Merrifield AL, Xie S-P (2016) Summer US surface air temperature variability: Controlling factors and AMIP simulation biases. J Clim 29:5123–5139
Min S-K, Kim Y-H, Lee S-M, Sparrow S, Li S, Lott FC, Stott PA (2020) Quantifying human impact on the 2018 summer longest heat wave in South Korea. Bull Am Meteorol Soc 101:S103–S108
Mora C, Coauthors (2013) The projected timing of climate departure from recent variability. Nature 502:183–187
Poli P, Coauthors (2016) ERA-20 C: an atmospheric reanalysis of the twentieth century. J Clim 29:4083–4097
Rodgers KB, Coauthors (2021) Ubiquity of human-induced changes in climate variability. Earth Sys Dyn 12:1393–1411
Schär C, Vidale PL, Lüthi D, Frei C, Häberli C, Liniger MA, Appenzeller C (2004) The role of increasing temperature variability in European summer heatwaves. Nature 427:332–336
Slivinski LC, Coauthors (2019) Towards a more reliable historical reanalysis: improvements for version 3 of the Twentieth Century Reanalysis system. Q J R Meteorol Soc 145:2876–2908
Stott PA, Stone DA, Allen MR (2004) Human contribution to the European heatwave of 2003. Nature 432:610–614
Swart NC, Coauthors (2019) The Canadian earth system model version 5 (CanESM5. 0.3). Geosci Model Dev 12:4823–4873
Tatebe H, Coauthors (2019) Description and basic evaluation of simulated mean state, internal variability, and climate sensitivity in MIROC6. Geosci Model Dev 12:2727–2765
Thompson DW, Barnes EA, Deser C, Foust WE, Phillips AS (2015) Quantifying the role of internal climate variability in future climate trends. J Clim 28:6443–6456
Wu T, Hu A, Gao F, Zhang J, Meehl GA (2019) New insights into natural variability and anthropogenic forcing of global/regional climate evolution. Npj Clim Atmospheric Sci 2:18
Yeh S-W, Won Y-J, Hong J-S, Lee K-J, Kwon M, Seo K-H, Ham Y-G (2018) The record-breaking heat wave in 2016 over South Korea and its physical mechanism. Mon Weather Rev 146:1463–1474
Yeo SR, Yeh SW, Lee WS (2019) Two types of heat wave in Korea associated with atmospheric circulation pattern. J Geophys Research: Atmos 124:7498–7511
Yoon D, Cha DH, Lee G, Park C, Lee MI, Min KH (2018): Impacts of synoptic and local factors on heat wave events over southeastern region of Korea in 2015. J Geophys Research: Atmos, 123, 12,081–012,096.